doi:10.1016/j.jmb.2010.12.008 J. Mol. Biol. (2011) 406, 195–204

Contents lists available at www.sciencedirect.com

Journal of Molecular Biology

journal homepage: http://ees.elsevier.com.jmb

Theoretical Analysis of Catalytic-sRNA-Mediated Gene Silencing

Yue Hao†, Liufang Xu† and Hualin Shi*

Institute of Theoretical Physics, Chinese Academy of Sciences, Beijing 100190, China

Received 29 April 2010;
received in revised form
17 November 2010;
accepted 1 December 2010
Available online
9 December 2010

Keywords:
small RNA;
noise;
RNA trap

Small regulatory RNA (sRNA) that acts by an antisense mechanism is critical for gene regulation at the posttranscriptional level. Recently, an Hfq-dependent sRNA named MicM, which is related to the regulation of outer membrane protein, was verified as a novel antisense sRNA due to its catalytic mode of regulation. Here we propose a simple kinetic model for the enzyme-like regulation mode of sRNA and study in detail the noise properties of the target gene under various recycling rates of the regulator. We predict that the recycling rate of sRNA and other relative parameters have significant influence on the noise strength of target expression. In comparison with the stoichiometric regulatory mode, a lesser fluctuation of target expression was observed near the threshold at which the transcription rates of both sRNA and target mRNA equal each other. We also found that the new mode is better in terms of rapid response to external signals. However, it needs more time to achieve target recovery if the stimulating signal disappears. Additionally, the obtained time evolution results of the MicM–*ybfM* interaction system based on our model are consistent with previous experimental results, serving as experimental evidence to back up our theoretical analysis.

Introduction

Small regulatory RNA (sRNA) is a type of noncoding RNA with typical length varying from ~50 nucleotides to several hundred nucleotides. As a crucial regulator, it is involved in many biological functions such as stress response,[1–4] quorum sensing,[5–7] and so on. Approximately 80 sRNAs have been verified[8] in *Escherichia coli*, most of which use an antisense mechanism by base-pairing with other RNAs.[1] These sRNAs are often induced under stress conditions and respond rapidly to environmental threat.[9,10] They are usually retained at a very low copy number, so stochastic effects can become prominent.

Numerous studies sought to understand the dynamic features of gene expression controlled by sRNAs that lead to coupled degradation.[11–14] Comparison of protein and sRNA regulators based on simulations drew the conclusion that regulation by sRNA is advantageous when a rapid response to an external signal is required. This is in consistent with experimental data.[12,14] Noise analysis indicated that the noncatalytic mode of gene regulation by sRNA has a unique feature in noise resistance.[12,14]

Different from the ordinary mechanism of base-pairing sRNA regulators that act stoichiometrically on their targets,[1] recent studies found that, in *Salmonella*, an sRNA named MicM leads to selective degradation of the sRNA–mRNA duplex.[15–17] Its binding to *chb* mRNA leads to coupled degradation of both sRNA and mRNA. For another target–*ybfM* mRNA, the sRNA part of the RNA duplex remained undestroyed. However, the mRNA part could not escape the fate of degradation. Experimental results indicated that MicM-mediated regulation requires Hfq protein to enhance RNA duplex formation[17–19]

*Corresponding author. E-mail address: shihl@itp.ac.cn.
† Y.H. and L.X. contributed equally to this work.

Abbreviations used: sRNA, small regulatory RNA; SSA, stochastic simulation algorithm; MFPT, mean first passage time.

and implied that one molecule of MicM can participate in the degradation of several molecules of *ybfM* mRNA.[15]

The catalytic characteristic of sRNA enriched our understanding of gene regulation: It is a fusion of the traditional mechanism of the sRNA regulator and enzyme catalysis. It is natural to ask whether this new mode of posttranscriptional gene regulation mediated by sRNAs is well suited for biological tasks and whether this mode of gene silencing is efficient in suppressing fluctuations in its target genes.

Here we propose a simple kinetic model for catalytic-sRNA-mediated gene silencing to investigate the noise properties of a target gene and the time evolution of the interaction system by Monte Carlo simulations. Some unusual features of this regulatory mode are found and compared with ordinary antisense mechanism. Catalytic sRNA is promising as a more effective regulator owing to its fast response ability and low recovery capability of target expression.

Results

A basic model for catalytic-sRNA-mediated gene silencing

Our theoretical study of catalytic-sRNA-mediated repression starts with a mass action model (Fig. 1). The minimal system consists of a single species of small RNA (s), a single species of mRNA target (m), the duplex (s_m) formed by the two species of RNA, and the protein product (p) of the mRNA. As a simplified model for catalytic sRNA, an sRNA can bind the 5′ untranslated region of an mRNA at its ribosome binding site to block translation initiation. In this model, we assume the following:

(1) Small RNA and its target mRNA are coded by independent genes using different promoters for their transcription. They are synthesized at rates α_s and α_m, respectively.
(2) The binding of sRNA to mRNA is irreversible and fast with the binding rate k, while an sRNA–mRNA duplex is degraded with the linear rate β_{sm}. A proportion of sRNA is successfully recycled as provider of sRNA regulators from the degraded duplex; the recycling ratio δ ranges from 0 to 1.
(3) Proteins are translated at a linear rate k_p off mRNA molecules, and each mRNA molecule produces on average of n protein molecules during its lifetime $\frac{1}{\beta_m}$, so $k_p = n\beta_m$.
(4) All molecules of sRNAs, mRNAs, sRNA–mRNA duplexes, and proteins, are subject to degradation with linear rates β_s, β_m, β_{sm} and β_p, respectively.

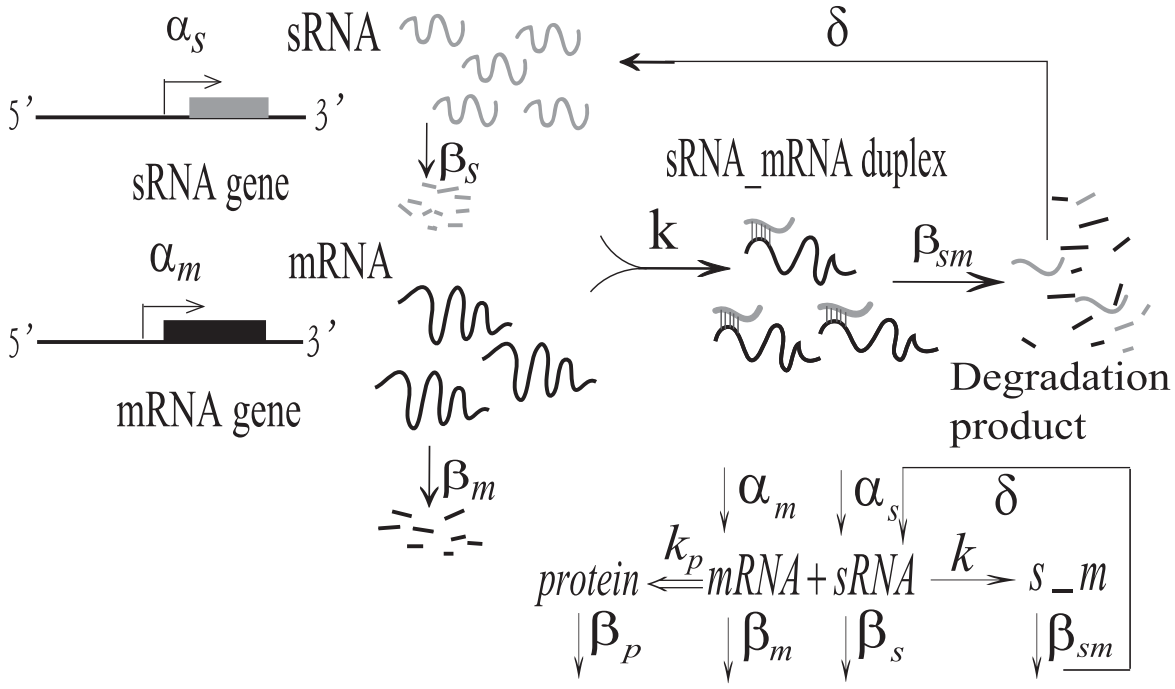

Fig. 1. Schematic diagram of catalytic-sRNA-mediated gene regulation.

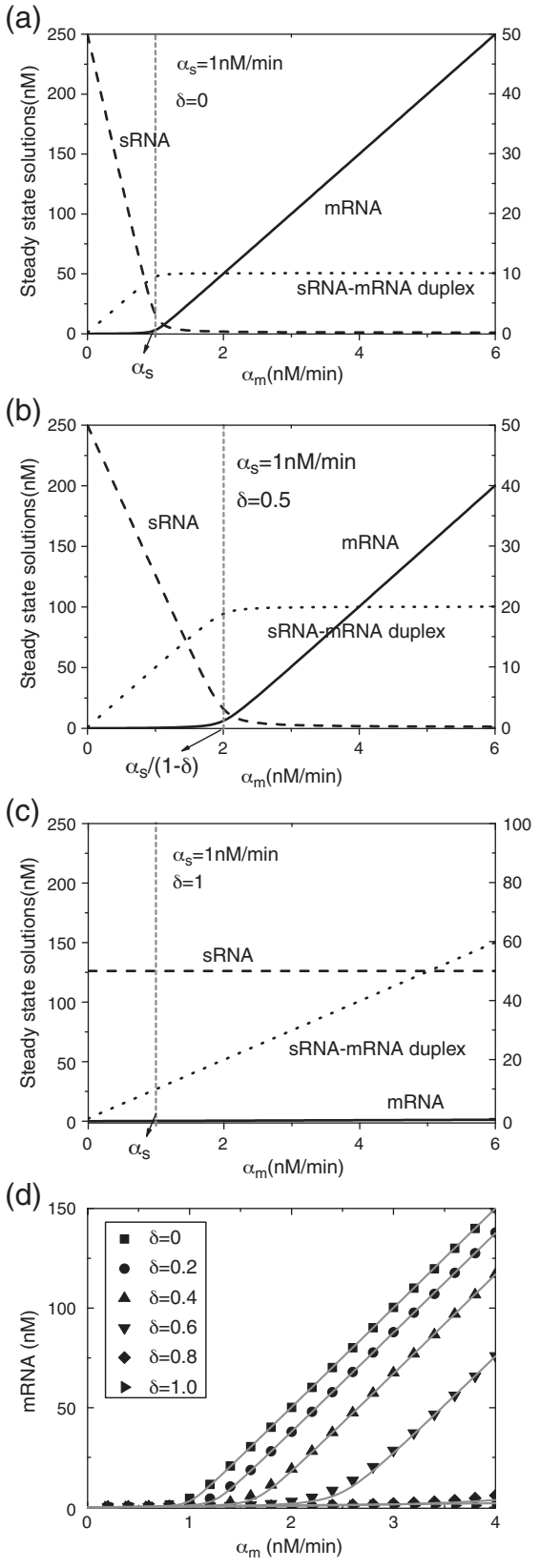

The process, as shown schematically in Fig. 1, can be quantitatively described with a system of differential equations:

$$\begin{aligned}\frac{ds}{dt} &= \alpha_s - \beta_s s - ksm + \delta\beta_{sm}(s\_m)\\ \frac{dm}{dt} &= \alpha_m - \beta_m m - ksm\\ \frac{d(s\_m)}{dt} &= ksm - \beta_{sm}(s\_m) - \beta_{gd}(s\_m)\\ \frac{dp}{dt} &= k_p m - \beta_p p\end{aligned} \tag{1}$$

Here, we assumed that the other proteins involved (Hfq, degradosome, etc.) are present at levels that are sufficient not to limit reaction rates. The degradation of all molecules is caused by direct degradation and growth dilution. Direct degradation of the sRNA–mRNA duplex will save a fraction of sRNAs, but growth dilution will not. In order to show this difference, we explicitly write the growth dilution term for the sRNA–mRNA duplex, where β_{gd} is related to the growth rate. Usually, direct degradation of the sRNA–mRNA duplex is much faster than growth dilution, and we neglect it in the ensuing discussion. The steady-state solutions for s and m can be deduced from the following equations:

$$\begin{aligned}\alpha_s - \beta_s s - k(1-\delta)sm &= 0\\ \alpha_m - \beta_m m - ksm &= 0\end{aligned} \tag{2}$$

For mRNA, the rate k here is the same as the coupled degradation rate in the previous stoichiometric mode[12] (Fig. 2a); however, for sRNA, part of the sRNAs (δksm) can be recycled from the

Fig. 2. Steady states with different recycling ratios. (a–c) Steady-state solutions of mRNA (left ordinate), sRNA, and sRNA–mRNA (right ordinate) with $\delta = 0$, 0.5, and 1, respectively. (d) The levels of target mRNA in steady state with different recycling ratios of sRNA. The lines are obtained from steady-state solutions (Eqs. (3) and (4)). The symbols are obtained from Monte Carlo simulations, where 10^6 steps of simulation were used for each recycling ratio δ. Parameters are set as $\alpha_s = 1$ nM min^{-1} and $k = 0.1$ (nM min)$^{-1}$. The other parameters are estimated from experiments.[15] We set $\beta_s = \beta_m = 0.02$ min^{-1} and $\beta_{sm} = 0.1$ (nM min)$^{-1}$. The half-lives of both sRNA and mRNA are about 27 min, and the half-life of the RNA duplex is about 4 min.[15]

degraded RNA duplex. Thus, the solutions under reaction equilibrium conditions are (for $\delta \in [0,1)$):

$$m^* = \frac{1}{2\beta_m}\left[\left(\alpha_m - \frac{1}{1-\delta}\alpha_s - \frac{\lambda}{1-\delta}\right) + \sqrt{\left(\alpha_m - \frac{1}{1-\delta}\alpha_s - \frac{\lambda}{1-\delta}\right)^2 + 4\alpha_m\frac{\lambda}{1-\delta}}\right]$$

$$s^* = \frac{1}{2\beta_s}\left[(\alpha_s - (1-\delta)\alpha_m - \lambda) + \sqrt{(\alpha_s-(1-\delta)\alpha_m-\lambda)^2 + 4\alpha_s\lambda}\right]$$

$$(s\_m)^* = \frac{\alpha_m - \beta_m m^*}{\beta_{sm}}$$

$$p^* = \frac{k_p}{\beta_p}m^* \qquad (3)$$

where $\lambda = \frac{\beta_m\beta_s}{k}$ is the leakage rate of mRNA expression[12] (Fig. 2a). The effect of the leakage expression rate of mRNA can be neglected, since the binding reaction is fast due to the participation of Hfq. In this study, k is set as 0.1 (nM min)$^{-1}$ to represent a fast combination between sRNA and mRNA. The catalytic mechanism maintains the characteristic of a "threshold-linear response."[12,20] The threshold here, however, is characterized by $\frac{1}{1-\delta}\alpha_s$, not by α_s. It rises as δ increases. Above the threshold, the mRNA level will start to increase linearly with this production rate α_m. It is obvious that at a fixed value of α_s, a higher recycling ratio of sRNA leads to a higher level of gene silencing (Fig. 2).

The sRNA of the degraded RNA duplex will be 100% recycled if $\delta = 1$, and the recycled sRNA will exert its effect again on other mRNA molecules. This process is similar to a protein regulator taking part in posttranscriptional regulation, which results in the degradation of target mRNAs. Taking limit $\delta \to 1$ in Eq. (3) or deriving directly, we have:

$$s^* = \frac{\alpha_s}{\beta_s}$$
$$m^* = \frac{m_0}{1 + \frac{k}{\beta_m}s^*} = \frac{m_0}{1 + \frac{\alpha_s}{\lambda}} \qquad (4)$$

where $m_0 = \frac{\alpha_m}{\beta_m}$ denotes the stationary level of mRNA in the absence of the regulator. Thus, the level of sRNA molecules remains constant even when α_m is varied, whereas the number of sRNA-mRNA duplex linearly increases with α_m (Fig. 2c). With parameters estimated based on experiments, mRNA is suppressed at a low level even when $\alpha_m \gg \alpha_s$ (Fig. 2d). It is interesting that the steady state of this mode is similar to that of protein-based transcriptional inhibition, which is characterized by $m^* = \frac{m_0}{1 + \left(\frac{r}{a}\right)^n}$. Here r is the concentration of the transcription factor, a is related to binding affinity, and n is the Hill coefficient.[21,22] It should be emphasized that, in both cases, the efficiency of regulators is closely related not only to the concentration of the regulator but also to the binding rate with its target. Catalytic sRNA interpolates between the conventional protein regulator and the sRNA regulator.

Description of noise strength

It is well known that gene regulation is intrinsically noisy due to the stochastic nature of underlying biochemical reactions.[12,20,23–25] In this article, we define intrinsic noise as fluctuations in mRNA number and output protein number at a fixed input of α_m, α_s, and so on.

The master equation for the distribution of the mRNA, sRNA, sRNA–mRNA duplex, and protein copies (m, s, c, and p, respectively) in this model is given by:

$$\frac{\mathrm{d}}{\mathrm{d}t}P(m,s,p,c) = \Big[\alpha_m\left(h_m^- - 1\right) + \beta_m\left(h_m^+ - 1\right)m + \alpha_s\left(h_s^- - 1\right) + \beta_s\left(h_s^+ - 1\right)s + k\left(h_m^+h_s^+h_c^- - 1\right)ms + \delta\beta_{sm}\left(h_s^-h_c^+ - 1\right)c + \beta_{sm}\left(h_c^+ - 1\right)c + k_p m\left(h_p^- - 1\right) + \beta_p\left(h_p^+ - 1\right)p\Big]P(m,s,p,c) \qquad (5)$$

where h^+ and h^- are, respectively, the lowering and raising operators defined through $h_x^+f(x) = f(x+1)$, $h_x^-f(x) = f(x-1)$, and $h_x^-f(0) = 0$ for any function $f(x)$. All time derivatives are set to zero here, as we focus on the steady-state properties of gene expression.

To describe noise strength, we use a sensitive measure of noise, the Fano factor, which is defined as $F_x = \frac{\sigma_x^2}{\mu_x}$ for stochastic variable x, where σ_x^2 is the variance and μ_x is the mean. For the Poisson process, the factor equals 1.

Dependence of noise strength on recycling ratio

It has been previously found that sRNA-based regulation is more efficient than transcription-factor-based regulation both in responding rapidly to signals and in filtering out noise from the environment.[12,20] Here we focus on the recycling rate of the sRNA regulator in the catalytic mechanism and quantitatively describe its influence on the noise strength of target expression.

It is difficult to directly solve the master equation describing the intrinsic stochastic behavior of small-RNA-mediated regulation, so we use the well-known stochastic simulation algorithm (SSA) Gillespie direct

method[26] to generate the stochastic trajectory of the regulation process and then analyze the characteristic of noise (see details in Materials and Methods).

The threshold-linear mode of gene expression regulated by ordinary antisense sRNA has been carefully analyzed. It has been concluded that the fluctuation of target gene expression depends largely on the ratio of the transcription rate of the target mRNA (α_m) to the transcription rate of the sRNA regulator (α_s).[12,20,27] A similar behavior is now also predicted for gene expression controlled by catalytic sRNA. Based on the master equation (Eq. (5)), the average number of mRNA or the first moment of m was drawn in Fig. 2d. The result shows that the average numbers of species provided by stochastic simulations are consistent with the solutions of the deterministic equation.

We present the relationship between the Fano factors of mRNA and the production rate α_m under different recycling ratios in Fig. 3a. It shows that the inflection points of these curves move rightward along the α_m axis. The peak position changes as $\frac{1}{1-\delta}\alpha_s$, and the peak value becomes larger as δ increases. Note that in the regime where the transcription rates of mRNA and sRNA are comparable, the value of the Fano factor decreases as δ increases. This result may be important in biological function, as is mentioned in the literature (that most actual biological parameters are near this point when sRNA silences its target gene). In other words, the catalytic-sRNA-mediated regulation mechanism tends to attenuate noise more than ordinary sRNA regulation when gene silencing happens. Due to the large stochastic fluctuation in the cell, it is important to ensure that the silencing function is reliable.

Protein noise has a similar behavior, except for $\alpha_m \gg \frac{1}{1-\delta}\alpha_s$ (Fig. 3b), where the Fano factor of protein approaches $1+\frac{b}{1+\frac{\beta_p}{\beta_m}}$ (equal to about 2 here) instead of 1. The same result can be deduced from the master equation in the following manner: Multiplying the master equation by m, m^2, s, and s^2, respectively, and summing over m, s, p, and c, with some approximations, we can derive that for $\alpha_m \ll \frac{1}{1-\delta}\alpha_s$ and $\alpha_m \gg \frac{1}{1-\delta}\alpha_s$, F_{m} indeed approaches 1. It was found that $F_p \approx 1$ for $\alpha_m \ll \frac{1}{1-\delta}\alpha_s$ and that $F_p \approx 1+\frac{b}{1+\frac{\beta_p}{\beta_m}}$ for $\alpha_m \gg \frac{1}{1-\delta}\alpha_s$, where $b=\frac{k_p}{\beta_m}$ is the average number of proteins produced from one transcript (called "burst size" by some authors).[20,23] The "burst" of protein in an mRNA translation process causes amplification of noise in gene expression, which has been elucidated in detail.[23,27]

A previous work on stoichiometric sRNA-mediated gene regulation[27] found that there is bimodality of target mRNA under certain parameters near the threshold, and the high correlation between sRNA and its target mRNA will form an effective potential barrier to shape the bimodal distribution. We also found bimodality in this catalytic-sRNA-mediated regulation mechanism, which needs to be tested by future experiments (Fig. 4).

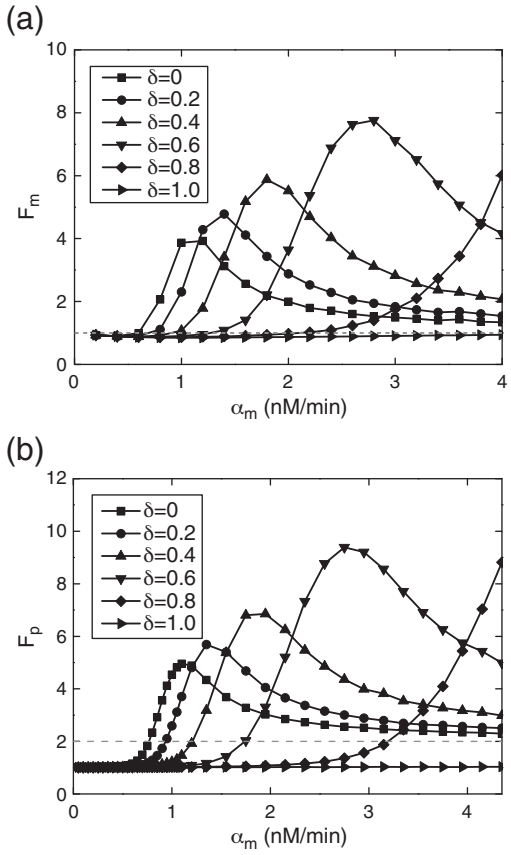

Fig. 3. Fano factors for target mRNA (a) and protein (b) with different recycling ratios. The gray broken line in (a) represents the Poissonian limit $F_{\mathrm{m}}=1$, and that in (b) represents the limit $1+\frac{b}{1+\frac{\beta_p}{\beta_m}}$. β_p is set to 0.02, and the other parameters are set as in Fig. 2. These results are obtained from 10^8 steps of Monte Carlo simulations.

Comparison between stoichiometric mode and full catalytic mode

We then focus on two limit cases in our model and find out their different behaviors. In our model (Eq. (1)), $\delta=0$ and $\delta=1$ correspond to a stoichiometric mode[27] and a fully catalytic mode, respectively. In a real biological system, degradation of the sRNA–mRNA duplex is caused by direct degradation and growth dilution. Direct degradation will save a fraction of sRNAs, but growth dilution will not. Thus, the recycling ratio of sRNAs will never exactly equal 1. But direct degradation is usually much faster than growth dilution, and δ is possibly close to 1. Thus, it is still helpful to study the behavior of the system at the limit case of $\delta=1$.

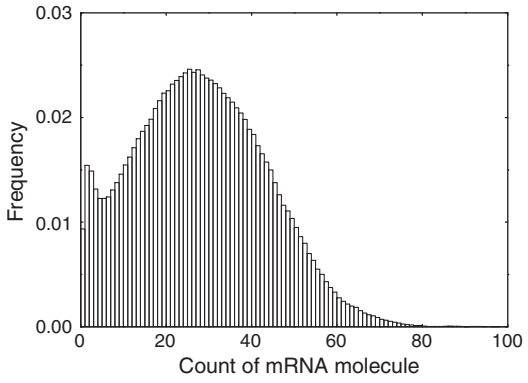

Fig. 4. Bimodal distribution of target mRNA. The parameters are set as: $\alpha_s=1$ nM min^{-1}, $\alpha_m=3$ nM min^{-1}, $\beta_s=\beta_m=0.02$ min^{-1}, $\beta_{sm}=0.1$ (nM min)$^{-1}$, $\lambda=0.0001$ nM min^{-1}, and $\delta=0.6$. The ordinate is scaled by the total number of mRNA molecules.

As $\delta=0$, it becomes the previous model that was studied in detail.[27] When $\alpha_m \ll \alpha_s$, almost all mRNA molecules will be targeted by small RNA, and only a thimbleful of mRNA, whose amount is not correlative to small RNA fluctuation, leak out. Alternately, when $\alpha_m \gg \alpha_s$, small RNA is used up, and the majority of mRNA is alive for translation. These two situations are close to the Poisson process, which leads the Fano factors' approach to 1 (Fig. 5, black line).

In the case of $\delta=1$, our result shows that the Fano factor remains close to 1, although the mRNA production rate (α_m) changes (Fig. 5). When $\alpha_m<\alpha_s$, the result is similar to Levine's model,[27] where mRNA molecules are mostly degraded, resulting in its fluctuation being irrelevant to small RNA fluctuation. While $\alpha_m>\alpha_s$, over quite a large range, mRNA will be consumed, as sRNA can remain at a constant level. The sRNA here can be recycled like an enzyme after the degradation of the mRNA–sRNA duplex. According to our simulations, F_m remains close to below 1 even when $\alpha_m \gg \alpha_s$.

To obtain a better understanding of full catalytic mode, we will return to deterministic results (Eq. (4) and Fig. 2c). It is obvious that more and more mRNA molecules will bind to sRNA molecules and then degrade as α_m increases. However, the level of free sRNA molecules stays the same because the effects of binding to mRNA and recycling from the duplex will cancel out each other. Small RNA pairing with its target mRNA produces a double effect: enhanced degradation of mRNA and protection from direct degradation (Eq. (4)). The latter effect enables sRNA to always satisfy the need for silencing by adjusting the level of the mRNA–sRNA duplex. That is, when $\delta=1$, although free sRNAs stay at the same level, the total sRNA concentration does increase with α_m, and this is why mRNAs are always repressed by sRNA and mRNA noise remains at a quite low level.

Influence of other parameters on noise

We analyzed the influence of the sRNA recycling rate on noise and found that a strong fluctuation of gene expression can be produced by a large δ. With fixed transcription rates (α_s and α_m), as more regulators are recycled, more targets will be influenced. It must be noted that sRNA recycling only happens with the degradation of the sRNA–mRNA duplex. Thus, the rate parameters of sRNA–mRNA duplex formation (k) and degradation (β_{sm}) should be considered as well. Here we give a quantitative view of how these parameters affect the noise of both mRNA and its protein product.

Figure 6a shows that noise is enhanced when the degradation of the duplex is enhanced. For certain recycling ratios, a fast degradation will speed sRNA recycling without changing the inflexion of the Fano factor curve, which is only decided by the recycling ratio. An upper limit of β_{sm}, above which sRNA recycling rates will not increase further, is expected. When $\beta_{sm}\simeq 0$, the model reduces to an ordinary sRNA-mediated model.[27]

Figure 6b shows how the binding rate k influences the fluctuation of output protein. We calculate the Fano factor of protein at a different binding rate k for $\delta=0.5$. Over a range of $\alpha_m<\alpha_s$, the Fano factor of the output protein decreases with increasing k. There are two limits of F_p, as the binding rate (k) is varied over a large range (from 0.0001 to 10 (nM min)$^{-1}$). When the process of binding is very fast, the few proteins produced for mRNA are fully repressed, and the noise curve approaches the Poissonian limit. For $k\simeq 0$, mRNA is freely translated, and the Fano factor approaches the limit of $1+b$ (≈ 2). In the silencing region, sRNA-based regulation can filter noise in the mRNA.[12] A larger binding rate k means

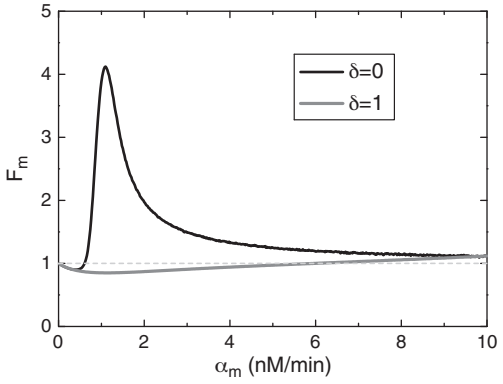

Fig. 5. Fano factors of mRNA for stoichiometric mode (black continuous line) and catalytic mode (gray continuous line). The light-gray broken line represents the Poissonian limit $F_m=1$.

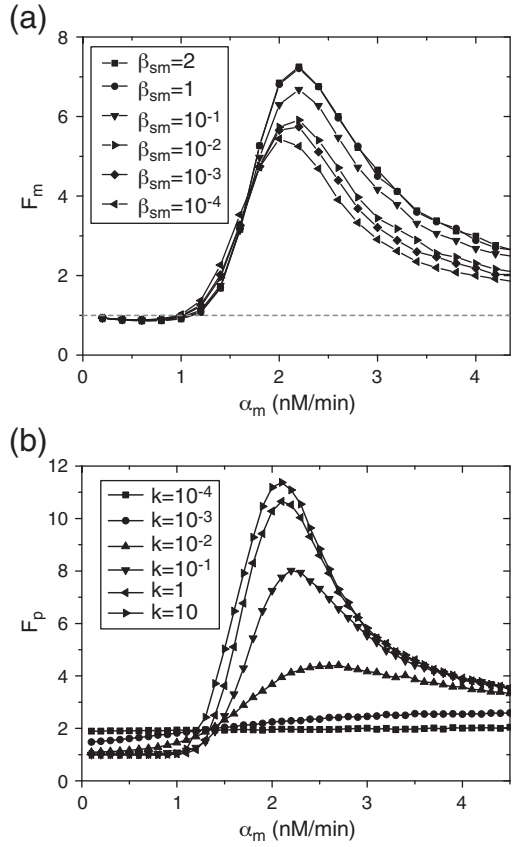

Fig. 6. Influence of β_{sm} and k on noise at a fixed recycling ratio $\delta = 0.5$. (a) F_m is affected by the degradation rate β_{sm} of the sRNA–mRNA duplex. (b) F_p is affected by the binding rate k. Here $\alpha_s = 1$ nM min^{-1}. All other parameters are set as in Fig. 2.

a more efficient sRNA, which leads to a smaller fluctuation of mRNA in the silencing region.

On the contrary, the result shows that over a range of $\alpha_m > \alpha_s$, a larger binding rate k of mRNA with sRNA produces a larger fluctuation of the output protein. At this region of α_m, the noise of sRNA will propagate to the mRNA, and the efficiency of noise propagation depends on the binding rate. As k approaches infinity, the number of free mRNA that can work for translation is the difference between the number of mRNA and the number of sRNA. Thus, it will keep all noise originating from mRNA and sRNA in the free mRNA. With a decreasing combination rate k, the coupling between mRNA and sRNA becomes weaker, and the noise of mRNA propagated from sRNA becomes smaller.

Response and recovery of target expression

It is important for a cell to be sensitive and to rapidly respond to an external signal. For the new sRNA regulation mechanism, the response time characterizes how long it takes for mRNA to change from an sRNA-free state to an sRNA-bound state. Below, we will use the mean first passage time (MFPT) to measure this important characteristic time.

Because of stochastic reactions and molecular fluctuation, it is necessary to calculate the time it takes to reach a new state in probabilistic meaning. The previous work provided information on response time through experiments.[15] However, solving the master equation to obtain an analytic result for response time is difficult. Here we still use the Gillespie direct method to solve the problem concerning both stochastic reaction and molecular fluctuation. From the results of Fig. 7a, we see that a faster response of the target always corresponds to a higher recycling ratio of the regulator. A smaller response time means a more sensitive and effective regulatory mode.

Recovery time is the time required for output recovery after the external signal has been removed. It is calculated similarly as the response time (see Fig. 7b). As the recycling ratio increases, the target mRNA will decrease, and more time will be

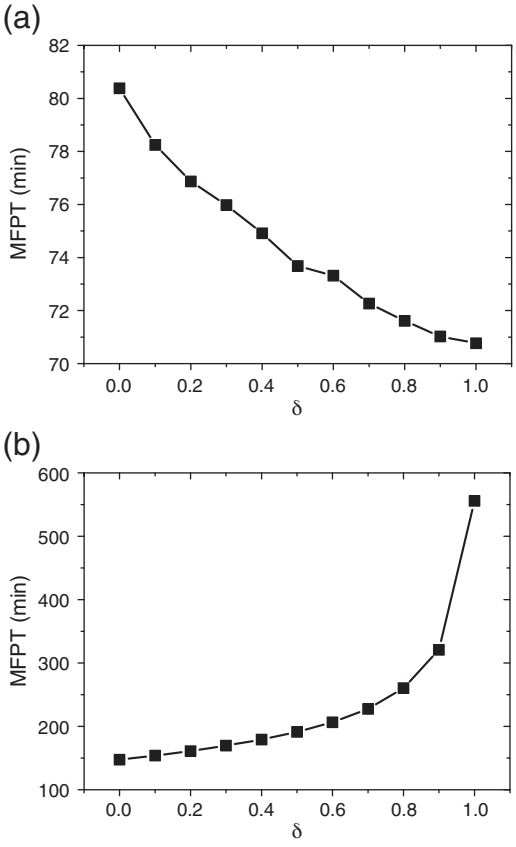

Fig. 7. Response time (a) and recovery time (b) of target gene expression. In the simulations, the threshold is set to 70% of the difference between the initial-state mRNA level and the final-state mRNA level. α_m is set to 0.5 nM min^{-1}, and the other parameters are set as in Fig. 2.

required for the recovery of this target gene expression. In the limit case of $\delta = 1$, the level of protein cannot recover from the repressed state even in several cell cycles (Fig. 7b). However, if the binding of the two RNA molecules or the degradation of the RNA duplex is slow and ineffective, the recovery of target expression may be fast even when the sRNA regulator is fully recycled.

Simulation results *versus* experimental results

To test our model, we simulate the time evolutions of sRNA and its target mRNA, respectively, when they are expressed alone and together in the system. As shown in Fig. 8a, according to our simulation with reasonable parameters, more than half of mRNA molecules are inhibited after 1 h of expression. For the fully recycling ratio $\delta = 1$, our simulation result shown in Fig. 8a is consistent with experimental results.[15]

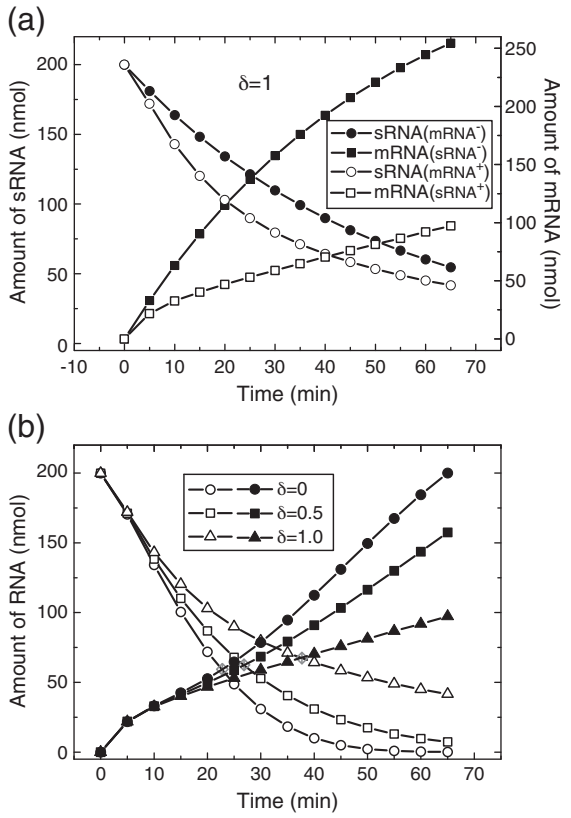

Fig. 8. Time evolutions of sRNA and its target mRNA. First, sRNA was expressed over 10 h to arrive at steady state. Then at time 0, the sRNA gene was shut off, and mRNA was expressed for 65 min. Parameters are set as: $\alpha_s = 4\ \text{nM min}^{-1}$, $\alpha_m = 7\ \text{nM min}^{-1}$, and $k = 0.001\ (\text{nM min})^{-1}$. Other parameters are set as in Fig. 2. (a) Time evolution of sRNA and mRNA with $\delta = 1$. Superscript "+" or "−" indicates the presence or the absence of relevant RNA, respectively. (b) Effects of δ on time evolutions. Empty symbols represent sRNA, and filled symbols represent mRNA.

We focus on the time point where the number of mRNA and the number of sRNA are equal to each other in a cell. After that point, mRNA continues to accumulate, while sRNA is still actively degraded (see Fig. 8b, gray rhombus). Consistent with the previous analysis, the more effective is the recycling, the more time it takes to reach the time point to start gene expression. Under the same condition, it takes twice as long for target mRNA to recover from the state of suppression with null recycling ($\delta = 0$) than with full recycling ($\delta = 1$).

Discussion

MicM was first proven to be an unusual antisense sRNA when it did not destabilize even when target *ybfM* mRNA was overexpressed. However, for another target gene that belongs to a *chb* operon and possesses complementarity to the same region of MicM, annealing of MicM causes coupled degradation.[15] For the most identified antisense sRNA-mediated gene silencing in bacteria, the Sm-like protein Hfq binds efficiently to both types of RNAs to stabilize them [17–19] and to accelerate annealing between them.[17,18] Here we start with a basic model of MicM–*ybfM* mRNA interaction and study in detail the noise properties of target expression by simulation. Our calculation shows that the inhibition effect of sRNA will be weak even with a high recycling rate (target mRNA will escape easily as k is reduced; data not shown). It implies that the inhibitory efficiency of catalytic sRNA depends more on the efficiency of sRNA–mRNA duplex formation than on the recycling ratio. On the other hand, it has been shown in Fig. 6b that a weaker binding between sRNA and mRNA usually causes more noise on target expression in the silencing region. All these findings may contribute to a better understanding of physiological significance and further design of the small RNA gene regulatory network.

It is interesting to note that all curves of mRNA in Fig. 2 can be considered equivalent if we scale α_s to $\frac{\alpha_s}{1-\delta}$ and if we scale λ to $\frac{\lambda}{1-\delta}$. In other words, the recycling ratio linearly affects the steady-state behavior of mRNA, but its influence on noise is distinctive; both the peak width and the peak value of the noise curve are significantly affected by the recycling ratio in a somewhat complicated manner, which will be considered in further studies.

It is known that sRNA is prevalent in bacteria, and it acts by various mechanisms besides base-pairing with other RNAs. For example, a few of the sRNAs are part of ribonucleoproteins that carry out specific housekeeping functions. Some others act by mimicking the structures of other nucleic acids to

sequester their cognate proteins.[8] All these regulatory modes are supposed to make sense in the selective evolution of life. Intricate regulatory information can be deciphered regardless of whether the regulator is a protein or an sRNA, the level of regulation, and whether the regulation is enzyme-like or not. In this sense, different noise performances may ensure life activity, diversity, and complexity.

Materials and Methods

The analysis was carried out using a simplified rate equation model and Monte Carlo (Gillespie algorithm[26]) simulations. All simulation parameters were obtained from a reasonable estimation of experiments.[12,15]

The Gillespie algorithm, developed by Daniel T. Gillespie in the 1970s, is well known as an effective SSA. By calculating the reaction probability density function $P(\tau,\mu)$ using the current reaction rate and reactant species combination number, we can determine the probability of when the next reaction will occur (τ) and which reaction will occur (μ). Then we renew the molecular number of relevant species. The Gillespie direct method needs two uniform random numbers to generate the random values τ and μ that obey the reaction probability density function, so it is also a type of Monte Carlo algorithm. In this way, we obtain statistically correct trajectories of the chemical system's time evolution, which is rigorously equivalent to that produced by the grand probability function $P(X_1,\ldots,X_N;t)$ as the solution of the master equation.

It is quite difficult to obtain an integrated analytic solution for even a simple master equation. The most important advantage of SSA is that it is an exact algorithm that takes full account of fluctuations and is easy to code in a computer program. It is also effective for calculating other relevant physical variables such as the Fano factor and response time.

Based on the ergodic hypothesis of equilibrium statistical physics, the ensemble average coincides with the time average (see Eq. (6)). To obtain the mean and variance of the molecules of a biochemical system, we only apply the frequency statistics (for a long-enough time) of the stochastic state sequence produced by SSA in steady state, with state waiting time as weight:

$$\langle X\rangle = \sum f(X)P(X) = \lim_{T\to\infty}\frac{1}{T}\int_0^T f(X(t))\mathrm{d}t \qquad (6)$$

where X represents the value of any reaction species here, and the function $f(X)$ may represent its mean value or variance.

We use a so-called MFPT to describe the response characteristic of the biochemical system. MFPT is defined as:[28]

$$\langle T_f\rangle = \int_0^\infty t(-\mathrm{d}P_t),\ \text{where}\ P_t = \sum_{X_i=0}^{Th_{X_i}} P(X_1,\ldots,X_N;t) \qquad (7)$$

Here, X_i is the variable of interest, and Th_{X_i} is its threshold value, while $\langle T_f\rangle$ represents its MFPT crossing the threshold. It theoretically represents the time it takes, on average, to reach a boundary the first time. The threshold values here mean certain boundary conditions. However, by simulation, we only use the stochastic state sequence produced by SSA and set a threshold value for the chemical reactant that we want to analyze and then calculate the time when it crosses the threshold the first time. Finally, we obtain the MFPT by averaging the results that are repeatedly derived.

Acknowledgements

This work was supported by the National Basic Research Program of China (grant 2007CB814800). H.S. is grateful to Zhongcan Ouyang, Weimou Zheng, and Terry Hwa for useful discussions.

References

1. Gottesman, S. (2004). The small RNA regulators of *Escherichia coli* roles and mechanisms. *Annu. Rev. Microbiol.* **58**, 303–328.
2. Majdalani, N. & Gottesman, S. (2005). The Rcs phosphorelay: a complex signal transduction system. *Annu. Rev. Microbiol.* **59**, 379–405.
3. Gottesman, S., McCullen, C. A., Guillier, M., Vanderpool, C. K., Majdalani, N., Benhammou, J. *et al.* (2006). Small RNA regulators and the bacterial response to stress. *Cold Spring Harb. Symp. Quant. Biol.* **71**, 1–11.
4. Vanderpool, C. K. (2007). Physiological consequences of small RNA-mediated regulation of glucosephosphate stress. *Curr. Opin. Microbiol.* **10**, 146–151.
5. Singh, P. K., Schaefer, A. L., Parsek, M. R., Moninger, T. O., Welsh, M. J. & Greenberg, E. P. (2000). Quorum-sensing signals indicate that cystic fibrosis lungs are infected with bacterial biofilms. *Nature*, **407**, 762–764.
6. Miller, M. B. & Bassler, B. L. (2001). Quorum sensing in bacteria. *Annu. Rev. Microbiol.* **55**, 165–199.
7. Lenz, D. H., Mok, K. C., Lilley, B. N., Kulkarni, R. V., Wingreen, N. S. & Bassler, B. L. (2004). The small RNA chaperone Hfq and multiple small RNAs control quorum sensing in *Vibrio harveyi* and *Vibrio cholerae*. *Cell*, **118**, 69–82.
8. Waters, L. S. & Storz, G. (2009). Regulatory RNAs in bacteria. *Cell*, **136**, 615–628.
9. Gottesman, S. (2005). Micros for microbes: non-coding regulatory RNAs in bacteria. *Trends Genet.* **21**, 399–404.
10. Aiba, H. (2007). Mechanism of RNA silencing by Hfq-binding small RNAs. *Curr. Opin. Microbiol.* **10**, 134–139.
11. Semsey, S., Andersson, A. M., Krishna, S., Jensen, M. H., Massé, E. & Sneppen, K. (2006). Genetic regulation of fluxes: iron homeostasis of *Escherichia coli*. *Nucleic Acids Res.* **34**, 4960–4967.
12. Levine, E., Zhang, Z., Kuhlman, T. & Hwa, T. (2007). Quantitative characteristics of gene regulation by small RNA. *PLoS Biol.* **5**, e229.

13. Shimoni, Y., Friedlander, G., Hetzroni, G., Niv, G., Altuvia, S., Biham, O. & Margalit, H. (2007). Regulation of gene expression by small non-coding RNAs: a quantitative view. *Mol. Syst. Biol.* **3**, 138.
14. Mitarai, N., Andersson, A. M., Krishna, S., Semsey, S. & Sneppen, K. (2007). Efficient degradation and expression prioritization with small RNAs. *Phys. Biol.* **4**, 164–171.
15. Overgaard, M., Johansen, J., Møller-Jensen, J. & Valentin-Hansen, P. (2009). Switching off small RNA regulation with trap-mRNA. *Mol. Microbiol.* **73**, 790–800.
16. Vogel, J. (2009). An RNA trap helps bacteria get the most out of chitosugars. *Mol. Microbiol.* **73**, 737–741.
17. Rasmussen, A. A., Johansen, J., Nielsen, J. S., Overgaard, M., Kallipolitis, B. & Valentin-Hansen, P. (2009). A conserved small RNA promotes silencing of the outer membrane protein YbfM. *Mol. Microbiol.* **72**, 566–577.
18. Mandin, P. & Gottesman, S. (2009). A genetic approach for finding small RNAs regulators of genes of interest identifies RybC as regulating the DpiA/DpiB two-component system. *Mol. Microbiol.* **72**, 551–565.
19. Sittka, A., Lucchini, S., Papenfort, K., Sharma, C. M., Rolle, K., Binnewies, T. T., Hinton, J. C. & Vogel, J. (2008). Deep sequencing analysis of small noncoding RNA and mRNA targets of the global post-transcriptional regulator, Hfq. *PLoS Genet.* **4**, e1000163.
20. Mehta, P., Goyal, S. & Wingreen, N. S. (2008). A quantitative comparison of sRNA-based and protein-based gene regulation. *Mol. Syst. Biol.* **4**, 221.
21. Bintu, L., Buchler, N. E., Garcia, H. G., Gerland, U., Hwa, T., Kondev, J. & Phillips, R. (2005). Transcriptional regulation by the numbers: models. *Curr Opin Genet Dev.* **15**, 116–124.
22. Bintu, L., Buchler, N. E., Garcia, H. G., Gerland, U., Hwa, T., Kondev, J. *et al.* (2005). Transcriptional regulation by the numbers: applications. *Curr. Opin. Genet. Dev.* **15**, 125–135.
23. Ozbudak, E. M., Thattai, M., Kurtser, I., Grossman, A. D. & van Oudenaarden, A. (2002). Regulation of noise in the expression of a single gene. *Nat. Genet.* **31**, 69–73.
24. Thattai, M. & van Oudenaarden, A. (2001). Intrinsic noise in gene regulatory networks. *Proc. Natl. Acad. Sci. USA*, **98**, 8614–8619.
25. Raser, J. M. & O'Shea, E. K. (2005). Noise in gene expression: origins, consequences, and control. *Science*, **309**, 2010–2013.
26. Gillespie, D. T. (1977). Exact stochastic simulation of coupled chemical reactions. *J. Phys. Chem.* **81**, 2340–2361.
27. Levine, E., Huang, M., Huang, Y. W., Kuhlman, T., Shi, H., Zhang, Z., Hwa, T. On noise and silence in small RNA regulation. Submitted. http://matisse.ucsd.edu/hwa/pub/sRNA-noise.pdf
28. Lan, Y. & Papoian, G. A. (2007). Stochastic resonant signaling in enzyme cascades. *Phys. Rev. Lett.* **98**, 228301.